Architecture, Structures and Construction (2025) 5:24
https://doi.org/10.1007/s44150-025-00137-3

RESEARCH

Revisiting structural Lazo carpentry: geometry, mechanics, and construction

Wesam Al Asali[1] · Ángel María Martín López[2] · Robin Oval[3] · Orsolya Gaspar[4] · Antonio José Lara-Bocanegra[5] · Almudena Majano-Majano[5] · Sigrid Adriaenssens[6]

Received: 2 November 2024 / Accepted: 4 March 2025 / Published online: 31 March 2025

Abstract
This paper explores the potential of traditional Spanish timber roofs as a structural system that blends framework carpentry with Islamic geometric patterns for contemporary construction. By integrating historical craftsmanship with modern engineering techniques, the research investigates solutions for spherical Lazo carpentry, where Lazo, or strapwork, designs fulfill both ornamental and structural roles. A key focus is the design, analysis, and fabrication of a four-meter-span Lazo pavilion, employing polyhedral projections to form modular spherical surfaces. Structural performance is evaluated through physical tests of materials and joints leading to an exploration of Finite Element Analysis (FEA) of the whole structure. The project also explores the construction and disassembly of the Lazo pavilion through defining the detailing of its different joints. The findings promise applications in spatial and shell structures, such as gridshells inspired by interlaced Lazo domes, providing a roadmap for designing structural Lazo discrete shells. Collaborating with architects, engineers, and master carpenters, this research enhances understanding across geometry, carpentry, structural mechanics, timber engineering, and architectural design while laying the groundwork for further exploration of this vernacular structural craft.

Keywords Timber structures · Carpintería de lo Blanco · Craft · Structural design · Discrete structures · Lazo · Islamic geometry · Grid shell

Introduction

Carpintería de lo blanco: definitions and historical terms

Traditional timber roofs, commonly known as *Artesonado*, are significant architectural features in the civil and religious buildings of the Ibero-American world. Originating from the fusion of Spanish-European structural carpentry and Islamic ornamental woodwork, these roofs thrived between the tenth and seventeenth centuries [1]. In the second half of the twentieth century, a body of scholarship revisited this craft by analyzing written treatises and built work. This review has opened the way for the making of new timber roofs, the documentation and restoration of existing ones, and the training of carpenters and designers on the craft [2–4].

The construction of these roofs, referred to as *Carpintería de lo Blanco*, encompasses two principal elements. The first is the *armadura*, or structural framework, which comprises essential components such as rafters, hip rafters, wall plates, ties, and joists (Fig. 1). Spanish carpenters employed a distinctive method known as plate construction, where prefabricated panels, or *paños*, composed of rafters and binders, were preassembled and then raised on the walls. These plates are unified by a horizontal element known as the *almizate*, typically placed in the central third of the rafters and characterized by repeated joists. Consequently, roofs in this tradition are defined by the number of plates to describe their section and their base to describe their plan: a gable roof is formed by two plates on

✉ Wesam Al Asali
wesam.alasali@ie.edu

✉ Robin Oval
R.Oval@tudelft.nl

1 IE University, Segovia, Spain

2 Escuela de Carpintería de lo Blanco de Narros del Castillo, Ávila, Spain

3 Delft University of Technology, Delft, the Netherlands

4 The Pennsylvania State University, State College, PA, USA

5 Universidad Politécnica de Madrid, Madrid, Spain

6 Princeton University, Princeton, PA, USA

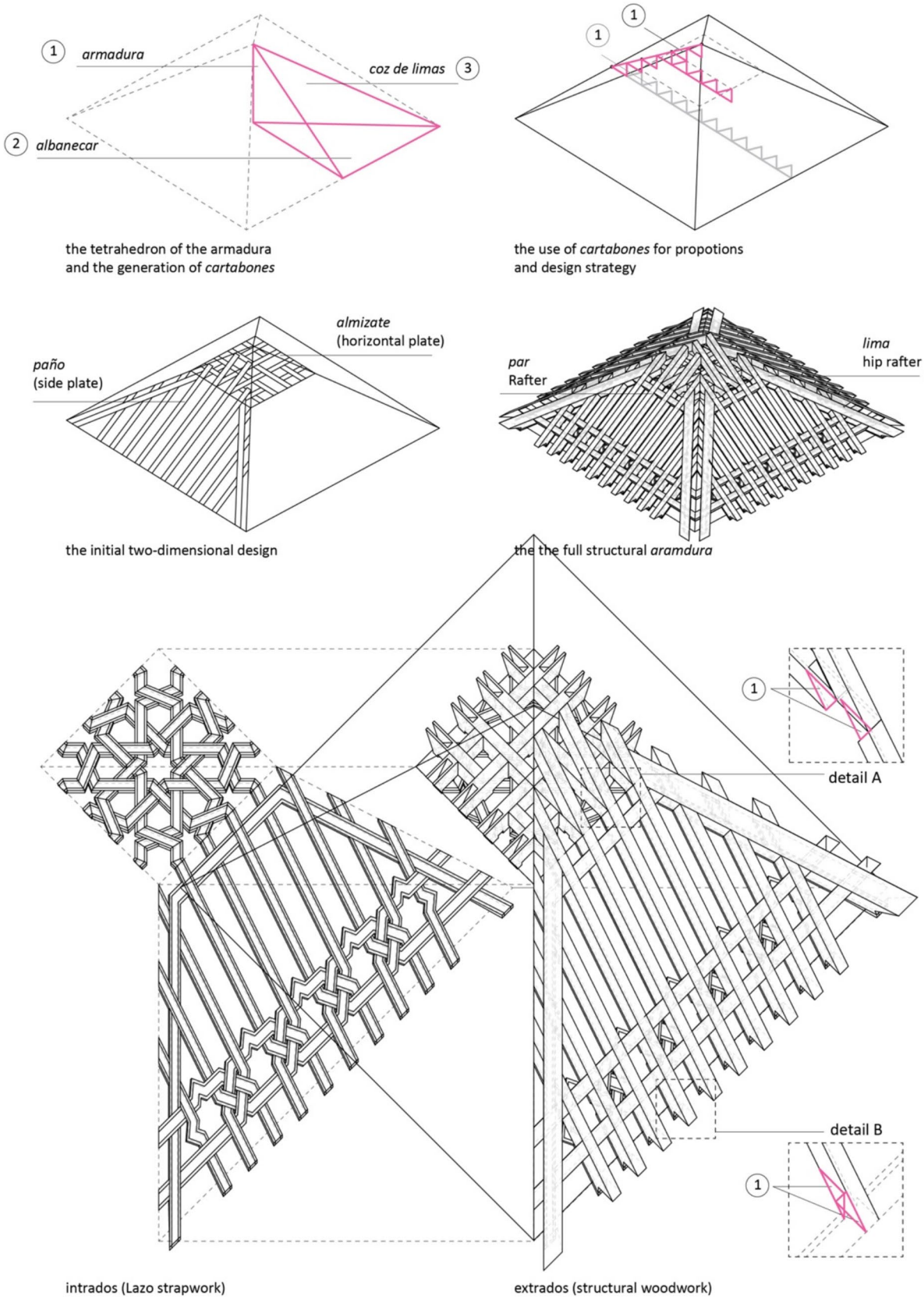

Fig. 1 An example of design and development of a timber roof with the craft of *Carpintería de lo Blanco* for a planar roof with square base (After Angel Maria Lopez Martin)

a rectangular base, while a bent pyramid roof consists of five plates on a square base, and so on. The second aspect of *Carpintería de lo Blanco* is the intricate wood strapwork known as *lacería*, which produces the Lazo that adorns the interior of the roof. This strapwork, inspired by Islamic geometric patterns, ranges from simple grids of repeating eight-pointed stars to complex configurations of varied rosettes arranged with symmetrical repetition. In some instances, Lazo is applied as cladding on boards affixed to the rafters. However, another traditional approach involves carving the structural elements themselves to create recesses that accommodate the decorative strapwork, seamlessly integrating ornamentation with structure (Fig. 2).

Therefore, the mastery of this woodwork lies in making the structural and decorative elements appear seamless. To integrate the pattern into the structure, the geometry of both must be harmonious. To achieve this, the craft of these roofs has developed a rich body of solutions based on geometrical rules of propositions of elements and angles of the joineries. These include the use of two sets of triangles, known as *cartabones*. The first set is used to determine the joinery of the structural elements, where three triangles, called *armadura*, *coz de lima,* and *Albanécar*, form a tetrahedron representing the rise of the ceiling, the rafter, and the hip rafter (Fig. 1). The second set of triangles guides the integration of the strapwork into the ceiling, where triangles correspond to the polygons of varied rosettes, such as hexagons, octagons, and so on. A well-designed interlaced timber roof should minimize irregularities in the strapwork across the structure, confining any inconsistencies to the intersections between the discrete plates.

The craft of structural interlaced timber roofs in Spain encompasses a rich lexicon, with specific terminologies for various parts of the structure. For example, a rosette is referred to as a *rueda de lazo*, or Lazo wheel. Each wheel is composed of intersecting bands that outline different polygons: the central star-shaped polygon is the *sino*; the small diamond-shaped polygons surrounding the star are the *almendrillas*; the elongated hexagons are the *azafates*; and the outer stars around the rosette are the *candilejos* (Fig. 2). The rosettes connect through the X-shaped part of the strapwork called *aspilla*. These terms are crucial not only in a

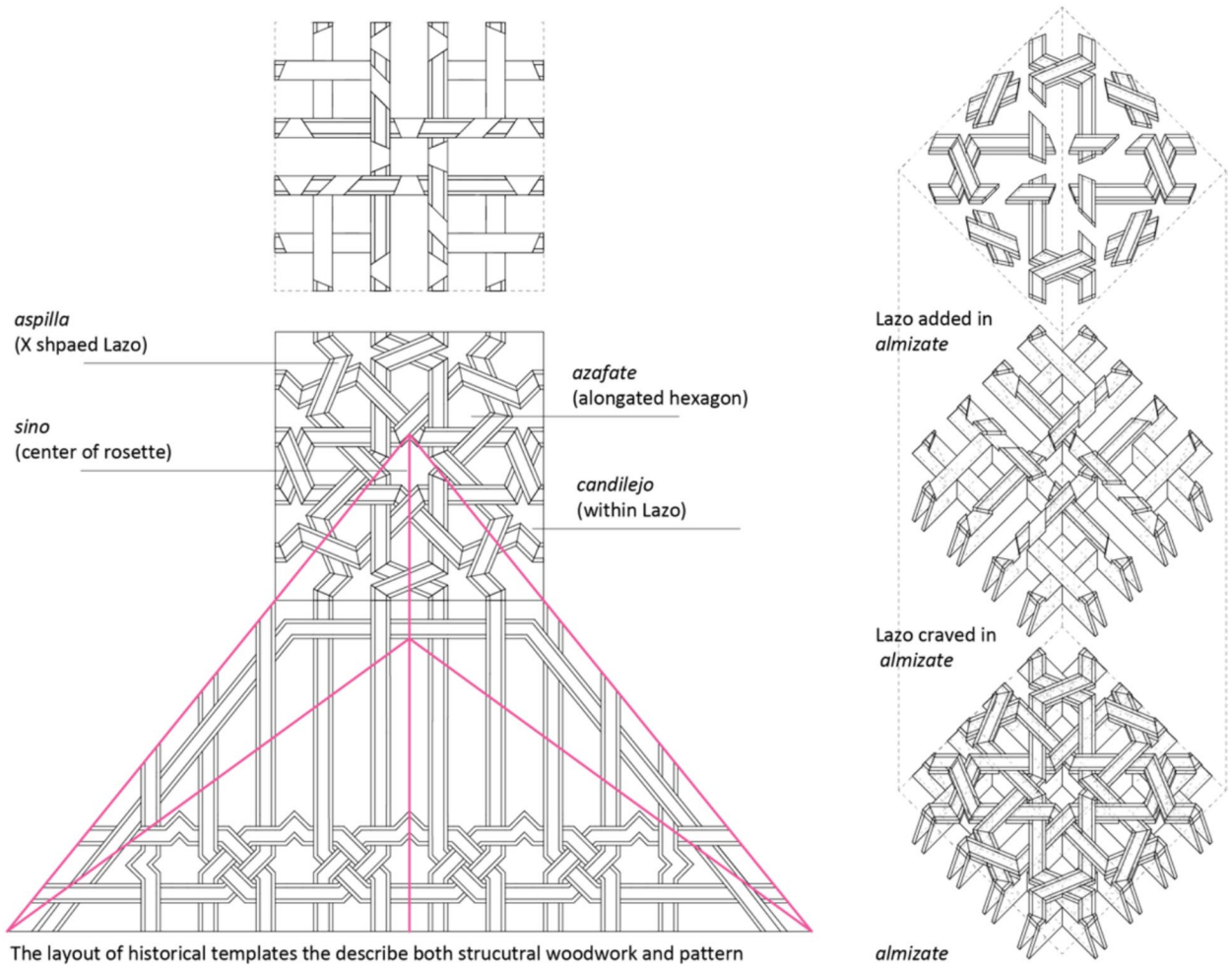

Fig. 2 The integration of the structure of the *armadura* with the design of the strapwork, Lazo (After Angel Maria Lopez Martin)

linguistic sense but also for developing and communicating structural and strapwork design solutions without relying on extensive drawings. Historically, and even in today's craft, what master carpenters produce as a design is often distilled into a template of the side face (*baño*) and the horizontal plan (*almizate*). These templates convey nearly all the essential information, such as pitch, proportions, and the design of the rosettes, necessary for constructing the roof.

From polyhedral to spheres: domical projections of Islamic geometry

Lazo carpentry has been heavily influenced by traditional Islamic geometric patterns. The subdivision patterns applied to domical surfaces are historically derived from the rich Islamic planar tiling tradition [5, 6]. Remarkably, in addition to regular (primarily six-fold) rotational symmetries, Islamic artists developed tilings featuring patches of "irregular" local rotational symmetries—particularly 5-, 8-, 10-, and 12-fold symmetries [7]. These symmetries manifest as convex (e.g., regular polygons) or concave polygons (star polygons like the rosettes) within the pattern, as seen in the application of *Girih* patterns [8]. For spherical timber surfaces, two fundamental questions arise regarding the projection of these patterns: (a) how the primary segments are defined (Fig. 3), and (b) how the pattern is projected onto those segments (Fig. 4). The first issue is referred to as projection, the second as subdivision.

While Spanish structural woodwork primarily features roofs made of planar surfaces, there are a few notable examples of wooden domes adorned with strapwork, such as those in the Royal Alcazar and the Casa de Pilatos in Seville, and the disappeared one in the Palacio de los Cárdenas in Torrijos [9, 10]. These domes, known as *media naranja* or half-orange domes, are constructed using meridian timber arches on the extrados. They are composed of 12 segments; each slice incorporates a projected orthogonal Islamic pattern featuring tenfold rosettes. Due to this meridian projection, zones of discontinuity in the pattern often appear at the edges or centers of each slice [10]. In these domes, the structural skeleton (the meridian arches) and the ornamental strapwork are distinct. This radial segmentation can also be found elsewhere, such as in the pointed masonry dome of the Friday Mosque at Golpayegan, Iran (1105–18) [6]. The other method of segmentation, the projection of spherical solids, or polyhedral projection, also known as geodesic design, is used in the third still existing historical example in Spain, the domes of the Palacio de Leones in Alhambra, Granada [8].

The polyhedral projection method is based on the central projection of a regular polyhedron (such as the five Platonic solids) or, less commonly, a semi-regular or another polyhedron onto the surface of its circumscribed sphere (Fig. 3) [11]. In terms of subdivision, in the Islamic tradition, designers leveraged the local (around vertices or faces), and the global symmetries of the polyhedra to align the patches derived from the planar tradition, such as rosettes of different folds [12]. For example, a vertex with five-fold symmetry would become the center of a pentagonal or decagonal tile. Therefore, certain polyhedra were used as a base geometry in the few examples of spherical projection across the tradition of Islamic patterns. For example, the dome of the Friday Mosque of Isfahan, Iran (1088–89) uses a pentagonal-faced dodecahedron, and the timber Mihrab of Madrasa al-Halawiyya in Aleppo, Syria (1245) uses an octahedron. These are two examples of Platonic solids being used as bases for spherical projection (Fig. 4). An example of an Archimedean solid is the truncated icosahedron (consisting of regular pentagonal and hexagonal faces) which was depicted in pictures of the lost Mihrab at Maqam Ibrahim El Sufi, also in Aleppo (1168). The afore-mentioned timber domes of Alhambra are unique in the sense that the segments are the projection of a distorted, octa-capped truncated icosahedron. Which is neither regular, nor semi-regular [13].

Aim: spherical Lazo carpentry

This paper aims to explore potential solutions for spherical Lazo carpentry where the strapwork design serves both ornamental and structural functions. For this aim, the study focuses on a design approach that divide spherical surfaces using polyhedral projections rather than meridian tessellations. The paper builds on the work of Ángel María Martín López, also a co-author of this article, who has developed several polyhedral projection solutions for Lazo domes and spheres [14]. This method creates modular spherical surfaces composed of repeated polygons that correspond to different rosettes, varying based on their number of folds. In addition to highlighting this possibility, the research aims to evaluate the structural behavior, constructability, and manufacturability of one of these solutions.

In the following section, this study introduces a proposal for a four-meter-span Lazo spherical tripod pavilion, serving as both a demonstrator and case study. By intersecting this polyhedral projection with the structural and aesthetic rules of Lazo carpentry, the design integrates joint strategy and construction methodology for the pavilion.

Subsequently, the research presents physical testing of the construction material, and an evaluation of various traditional lap joints used in Lazo carpentry. Based on the testing results, the tripod design is then analyzed through structural modeling using Finite Element Analysis (FEA).

Lastly, the research details the off-site fabrication of modular spherical triangles and the on-site assembly process. This includes fabricating the curved elements, tracing and

		Platonic		Archimedean
general properties	spherical?	circumscribed, middel, inscribed		circumscribed, middle, ~~inscribed~~
	regular?	all faces are congruent all faces are regular polygons all vertices have the same degree		~~all faces are congruent~~ all faces are regular polygons all vertices have same degree
	dual	Platonic solid		Catalan solid
example, specific properties	name	octahedron	dodecahedron	truncated icosahedron
	circumscribed sphere	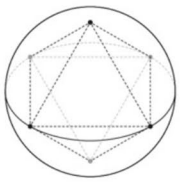 all vertices are on the sphere	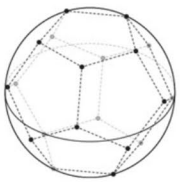 all vertices are on the sphere	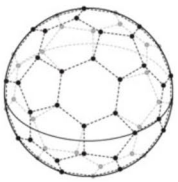 all vertices are on the sphere
	natural equator	true	false	false
	faces	8 triangles	12 pentagons	12 pentagons 18 hexagons
	vertices	20	20	30
built example	example	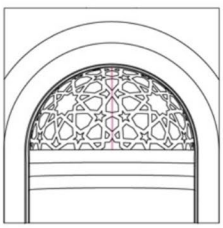  Halawiyya Mihrab Halawiyya Mosque, Aleppo	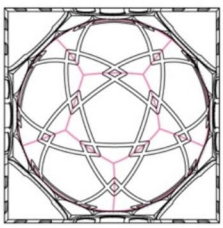  Taj-Al-Mulk Dome Jame' Mosque of Isfahan	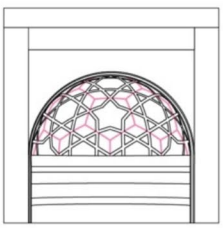 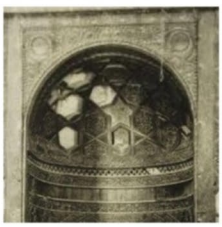 Mihrab Ibrahim al-Sufli, Aleppo

Fig. 3 Historical spherical Lazo examples I: Projections of Polyhedra on domical surfaces

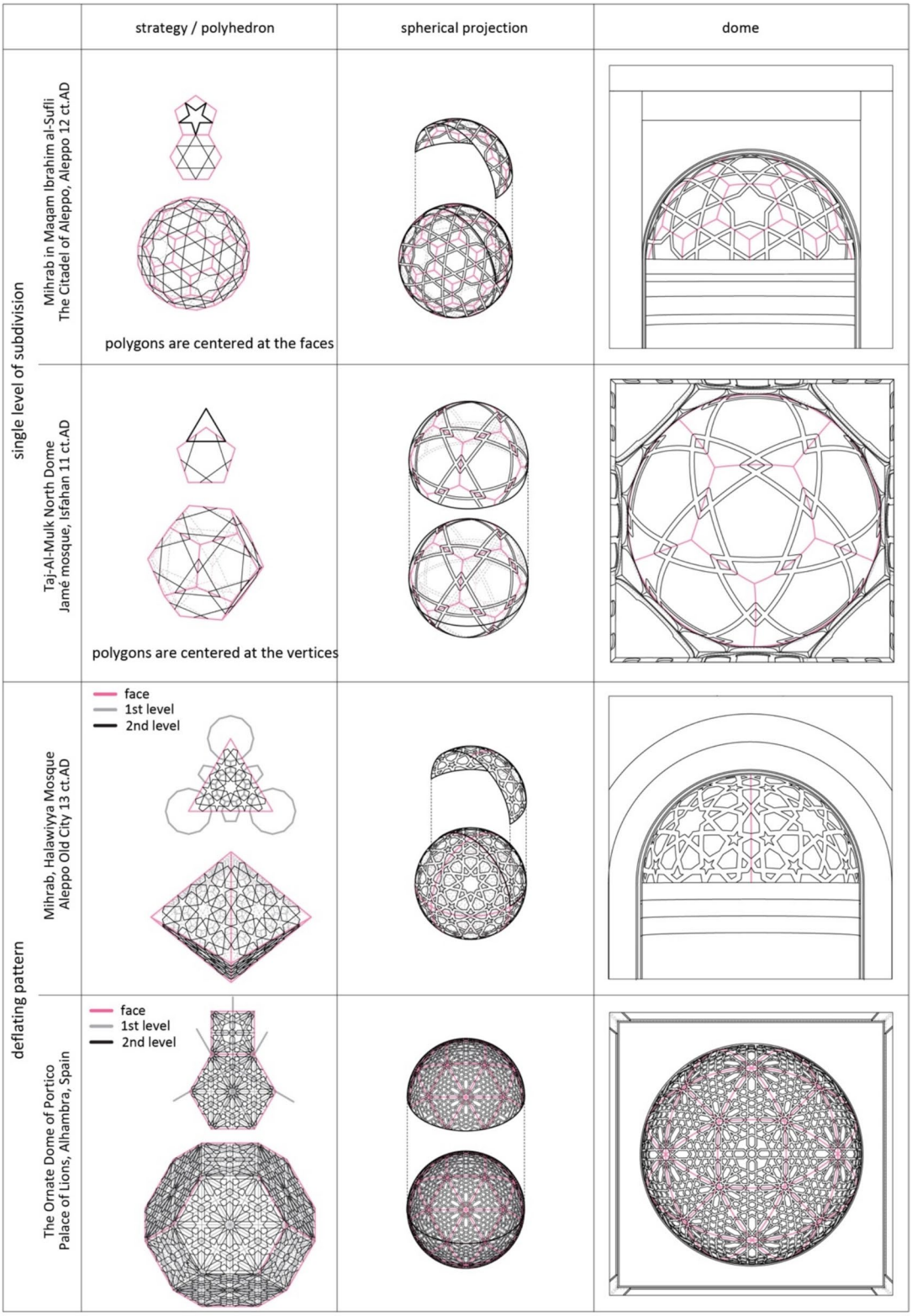

Fig. 4 Historical spherical Lazo examples II: subdivision of domical surfaces into Islamic pattern

crafting the joints, initial assembly of the spherical triangles, and the full on-site construction sequence.

The research holds promises for applications in spatial and shell structures, such as gridshells inspired by the interlaced Lazo domes. It aims to outline a roadmap for the design, construction, and application of structural Lazo discrete shells, composed of straight or curved, solid or laminated members based on easy-to-follow templates that outline different types of joints. The structural analysis of the various interlaced pattern solutions will be enlightening, as the behavior of these structures is not well known. The construction of a Lazo pavilion based on modular spherical triangles will also be relevant for timber shell construction literature.

Conducted as a collaboration between architects, engineers, and master carpenters, this research incorporates insights from multiple fields, including geometry, carpentry, structural mechanics, timber engineering, and architectural design while laying the groundwork for further exploration of this vernacular structural craft.

Lazo pavilion: design and crafts approaches

Projections and subdivisions

The polyhedron used in our research is the pentakis dodecahedron, which belongs to a special class of polyhedron of Catalan solids, the duals of Archimedean solids (Fig. 5). The reason of proceeding with this strategy was to archive a high level of modularity. The uniformity of the segments proved to be a significant advantage. The pentakis dodecahedron is composed of 60 congruent isosceles triangular faces. The dome (from which the tripod pavilion was derived) is projected using 30 identical spherical triangular segments. Each triangular segment was further subdivided with rosettes and stars, resulting in a repetitive pattern across the dome.

The triangulation of the spherical surface offers structural benefits [11]. However, our approach had to diverge from pure triangulation due to the ornamental traditions and fabrication considerations. In a pentakis dodecahedron, either 5 or 6 triangles converge at a vertex, creating complex joints that present challenges for wooden carpentry. The local 5- or sixfold rotational symmetries are matched with 10- and 12-pointed rosettes, respectively. This arrangement creates a quadrangular void between the triangles. This reinterpretation of the original spherical polyhedron generates an interwoven pattern that is inherent to Islamic tradition and is better suited for the craft of Lazo carpentry, foreshadowing the use of half-lap joints [5, 12].

Unlike Platonic regular solids, Catalan solids are not regular. This has benefits and downsides for our design. One benefit that our pavilion design leverages is congruent triangulation. A pentakis dodecahedron has three times more congruent triangular faces than the most subdivided Platonic solid (icosahedron) (Fig. 5). This level of segmentation results in a closer approximation of the spherical surface and the originally straight bars within the individual segment, needed to be bent less which results in easier fabrication. The other benefit of the pentakis dodecahedron comes from the distortion of its faces during projection: Catalan solids are not spherical, as not all their vertices lie on a single circumscribed sphere. This means that while they can be projected onto a spherical surface, their faces will be distorted. In the case of the pentakis dodecahedron used in our pavilion's design, this distortion causes its isosceles triangle planar faces to become closer to equilateral spherical triangles (The ratio of the longest to shortest edge is closer to 1 in the spherical triangles than in the planar triangles). This

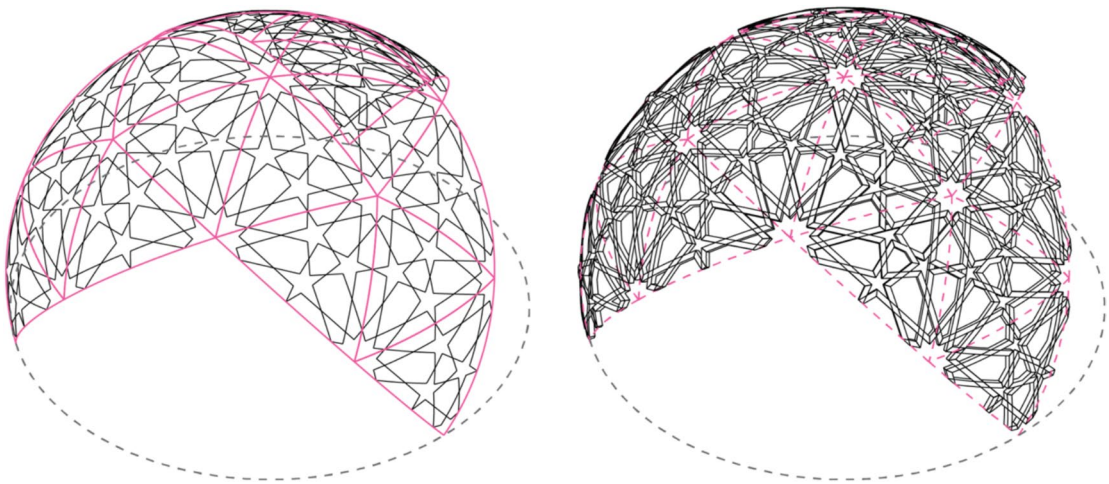

Fig. 5 Lazo pavilion proposal based on a pentakis dodecahedron. Left: wireframe model. Right: Thickened construction model

creates an aesthetic appeal, as people perceive regularity as more harmonious [15].

Craft rules and joints strategy

The transition from the wireframe model of the Lazo pavilion's pattern and arrangement to the construction model required careful consideration of specific craft rules. The first set of these concerns aesthetic and constructional rules of Lazo carpentry. These rules are normally applied in the planar Lazo carpentry and there were used in the subdivisions and drawings of the patterns on the pentakis dodecahedron. The rules that concern our Lazo pavilion design is the following (also illustrated in Fig. 6):

- **Canonical Layout of the rosettes:** The rosettes, or Lazo wheels, should always have parallel arms extending from the central polygon of the rosette. In planar Lazo carpentry, this parallelism is required as they rosettes arms usually conform to the location of the main structural elements, such as rafters and collars.
- **Discontinuities in Strapwork:** The intersecting bands in the strapwork cannot extend continuously across the polygons, especially within the *sino*. This limitation creates a challenge when the strapwork has a structural function, as many of the structural members will experience discontinuities.

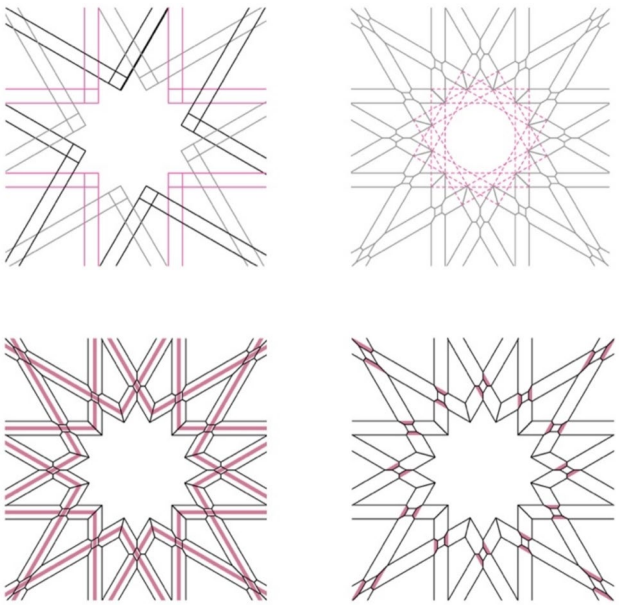

Fig. 6 Aesthetic and fabrication rules in planar Lazo carpentry that were adopted and employed in the design development of the Lazo pavilion. Top left: the arms of rosettes are parallel. Top right: The Lazo cannot extend in the central polygon. Bottom left: the intrados interlacing though colors. Bottom right: the denting in the joints to enhance the interlacing effect

- **Flat Intrados Surface:** The *intrados* surface of the strapwork bands must remain flush at the same level. The interlacing effect is achieved through the arrangement of the joints, with the bands alternating between continuation and interruption. This requires lap joints at the intersections between the elements.
- **Enhanced Aesthetic through Denting:** The interlacing effect is further emphasized by carving a dent, known as *emboquillado*, into the joints between the bands. This dent follows the direction of the crossing lazo and typically has a depth between one-quarter and one-fifth of the band's width.

These rules directly affect the constructability of the pavilion, introducing several key limitations to the timber gridshell structure. For instance, the Lazo pattern disrupts the continuity of the curved elements in the pavilion, creating discrepancy between adhering to structural intuition and respecting the craft's constraints. Additionally, the denting in the joineries introduces both structural and constructional advantages and disadvantages, which will be discussed in the following section. These craft rules were adopted and prioritized in the design of the pavilion.

The second set of rules were, in fact, the research aspirations for Lazo carpentry. What distinguishes the design strategy of the proposed division method from the historical examples is that, in this pavilion, the Lazo is conceived as structural. Unlike traditional designs where the ornamental strapwork is separate from the structural framework, the proposed approach in this paper integrates the two. The second aspiration is to make a dismountable Lazo pavilion, where the individual pieces can be disassembled when needed.

From the two sets of regulations, the resulting design of the Lazo pavilion consists of modular spherical triangles that repeat to form a structural Lazo configuration. These triangles feature two distinct types of joineries. The first set, located within the triangles, are glued lap joints that are permanently fixed and cannot be disassembled. The second set consists of the joineries connecting the triangles, which utilize a bolt and nut system (Fig. 7).

This design and strategy of joinery promises several advantages: the dome's lace is visible both on the extrados and intrados; the pavilion can be assembled and disassembled, especially when the modular unit of the dome is repeated; and the pavilion is reconfigurable, allowing it to be shaped and reshaped in different forms based on the arrangement of the modular units (Fig. 8).

Lazo tripod structural analysis and testing

The mechanical behavior of the Lazo tripod was assessed to help the designers and builders gain confidence during the design process regarding the types of joints and the

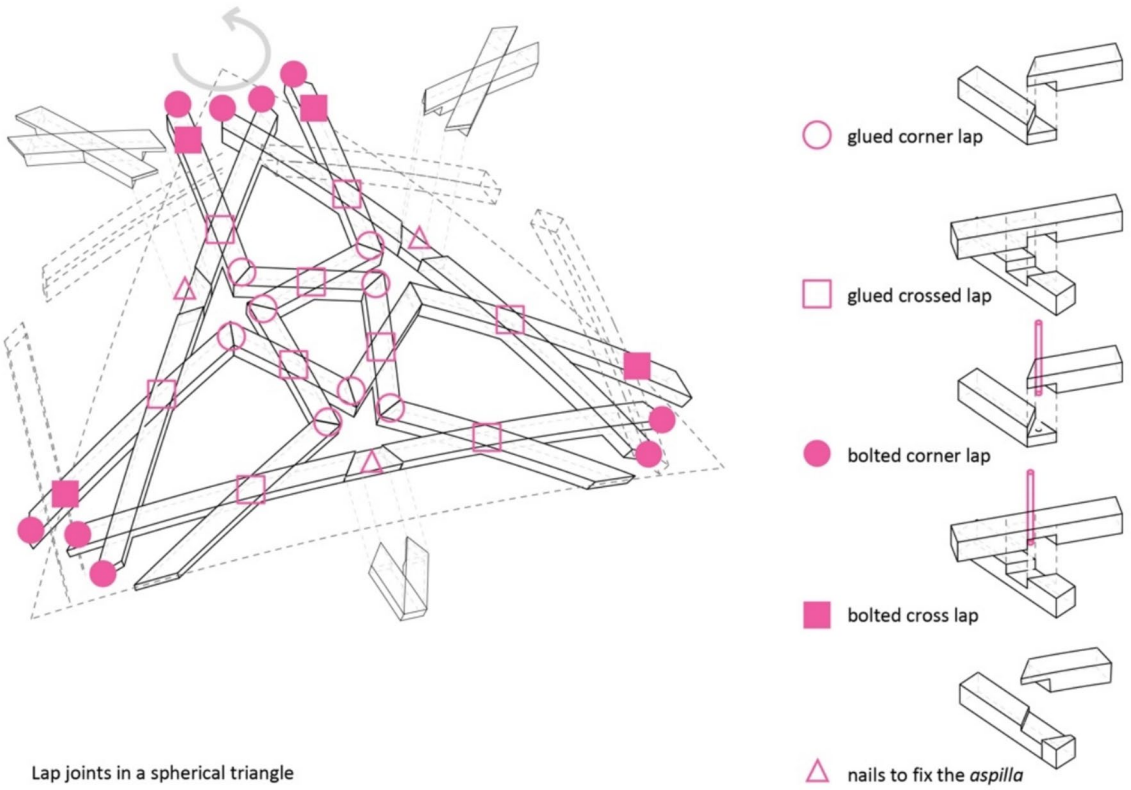

Fig. 7 The spherical triangle I: the main unit of the Lazo pavilion showing the strategy of assembly and joints. The joint inside the spherical triangle is glued, the joints between the spherical triangles are with bolts and nuts

potential need for additional stiffening. Indeed, connections play an important role in the behavior of timber structures, particularly in complex systems with multiple members and joints, such as grid structures [16], particularly a Lazo pattern, which favors bending moments. Physical tests were performed at the joint level first to inform a numerical model at the structural level. The material for the glued laminated timber beams is *Pinus sylvestris* from Spain with an average density of 558 kg/m^3. The beams have a thickness and a width of 40 mm. This material and the cross-section are the same as those used in the Lazo tripod.

Joint testing

The Lazo tripod is composed of timber elements with simple curvature, assembled using half-lap joints at various angles. While current standards provide guidelines for estimating the stiffness and strength of dowel-type connections, there is limited (or no) information on how to account for the stiffness of carpentry joints [17], making physical testing necessary to obtain reliable data. In addition, it is common for the strength and stiffness of dowel-type connections to vary depending on the orientation of the load [18]. The experimental work aims to provide an assessment of the effect of cross-sectional reduction at the half-lap joints on the bending strength and stiffness of timber members, considering the orientation of the load. This information serves as a basis for the development of a numerical model of the whole tripod.

The specimens were tested under bending, oriented in a manner consistent with the deformation they would have in the tripod due to out-of-plane bending moments, which were expected to be the most significant based on preliminary structural analysis. For this purpose, a four-point bending configuration under displacement control according to EN 408:2011 [19] was applied. The test span was set to 720 mm (18 h). Displacement at mid-span was measured using a transducer. Two types of lap joints were evaluated (Fig. 9): glued lap joints, representing the internal connections within the modules; and bolted lap joints, designed as reversible connections between the modules to facilitate assembly and disassembly.

For both types of lap joints, two notch positions were tested corresponding to the positive and negative moments that the tripod experiences under different load cases (Fig. 10): the notch located at the top, corresponding to a situation where the notch closes, so the cross piece provides some resistance; and the notch located at the bottom,

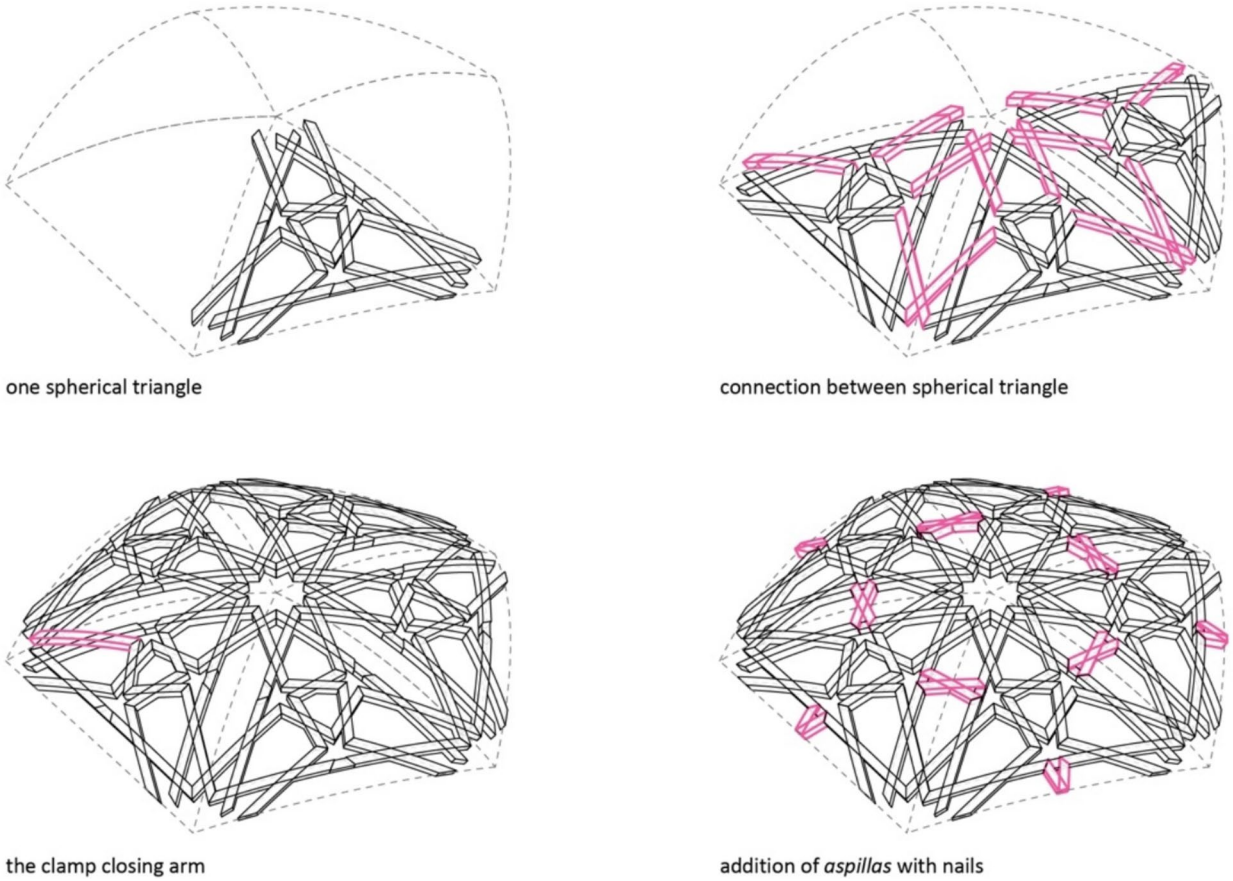

Fig. 8 The spherical triangle II: the repetition, joints, and assembly of the spherical triangle of the Lazo pavilion

Fig. 9 Bolted lap joint (left) and glued lap joint (right)

corresponding to a scenario where the notch opens, so the cross piece provides no resistance. Elements without joints with a full cross-section of 40×40 mm^2 were also tested to establish reference values for the material.

A total of eight specimens without joints were tested, along with four bottom-notched and two top-notched specimens for each group of glued and bolted lap joints.

Figure 11 displays the relationship between maximum bending moments and mid-span displacements for the elements without joints and for the various joint configurations.

Table 1 shows the mean and minimum values of modulus of elasticity and ultimate moment for the different groups of tests. For notched member, the modulus of elasticity represents the apparent modulus of elasticity, which includes the reduction in stiffness due to the notch.

The mean modulus of elasticity of the jointless elements was found to be approximately 15 GPa. In the case of glued lap joints, notching reduced the apparent modulus (Gj/Wj) to 62% for top notches and to 64% for bottom notches, representing slightly less than 2/3 of the modulus of the elements without joints. However, bolted lap joints exhibited a more substantial reduction, dropping to approximately 1/4. It therefore seems

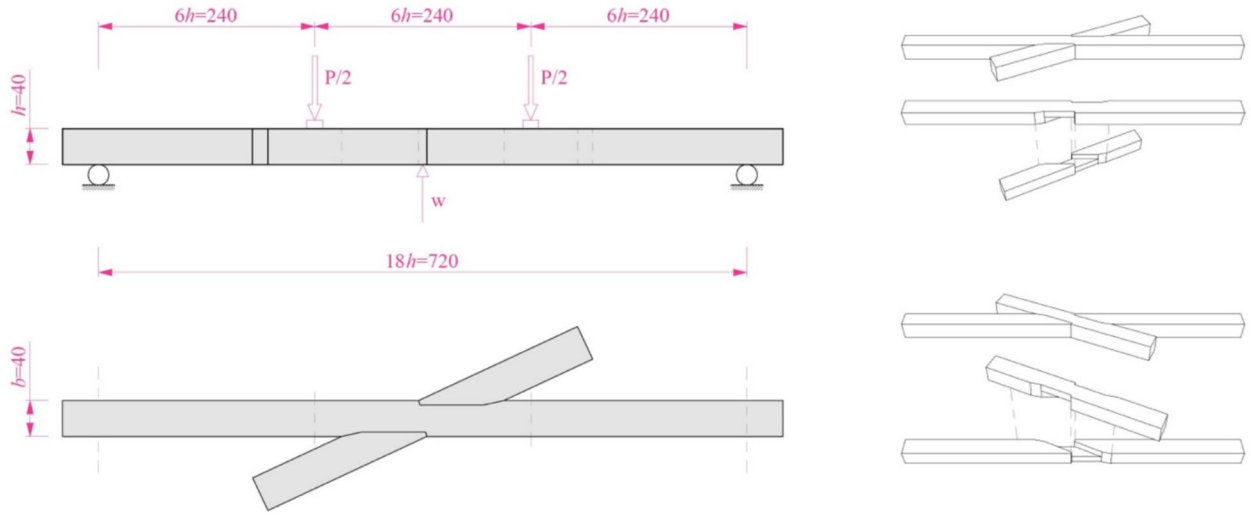

Fig. 10 Left: Plan and elevation views of a top-notched specimen; Right: exploded views of a top-notched joint (top) and a bottom-notched joint (bottom)

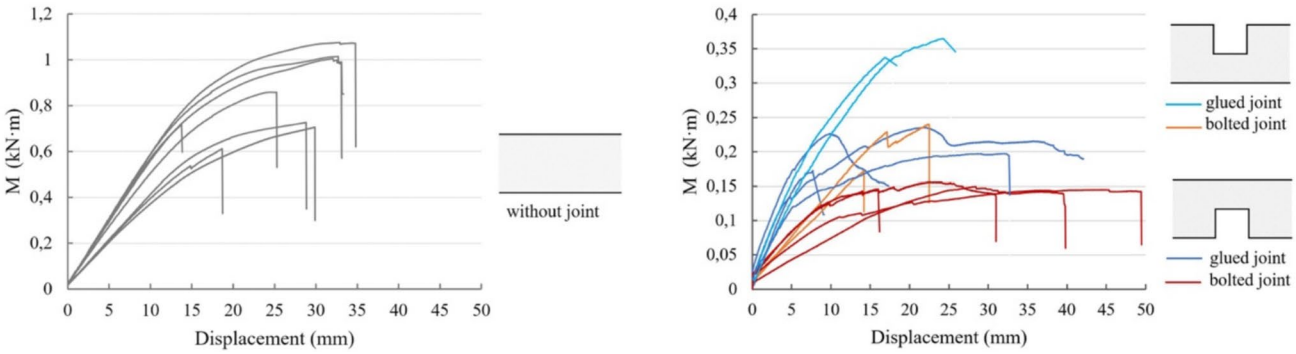

Fig. 11 Maximum moment (M) versus displacement curves of specimens without joints (left) and specimens with glued and bolted lap joints with top and bottom notch positions (right)

Table 1 Mean and minimum values of modulus of elasticity (E_0) and ultimate moment (M_u) for the members without joints and members with glued/bolted lap joints

	Without joint (Wj)	Glued lap joint (Gj)						Bolted lap joint (Bj)					
	All	All		Top notch		Bottom notch		All		Top notch		Bottom notch	
	(N/mm^2)	(N/mm^2)	Gj/Wj	(N/mm^2)	Gj/Wj	(N/mm^2)	Gj/Wj	(N/mm^2)	Sj/Wj	(N/mm^2)	Sj/Wj	(N/mm^2)	Sj/Wj
$E_{0,mean}$	14,941	9429	0.63	9229	0.62	9529	0.64	4107	0.27	4253	0.28	4010	0.27
$E_{0,min}$	11,356	6514	0.57	8457	0.74	6514	0.57	3280	0.29	3784	0.33	3280	0.29
	(kNm)	(kNm)	Gj/Wj	(kNm)	Gj/Wj	(kNm)	Gj/Wj	(kNm)	Sj/Wj	(kNm)	Sj/Wj	(kNm)	Sj/Wj
$M_{u,mean}$	0.84	0.25	0.30	0.35	0.42	0.21	0.25	0.16	0.19	0.21	0.25	0.15	0.18
$M_{u,min}$	0.61	0.17	0.28	0.34	0.55	0.17	0.28	0.12	0.19	0.17	0.28	0.15	0.24

From the tests conducted on full cross-section timber members, an average strength of approximately 72 N/mm^2 was obtained, with the minimum value around 53 N/mm^2

important to consider in the numerical models the significant reduction in stiffness caused by the lap joints, as this reduction leads to greater deformations and higher risks of buckling.

Regarding the ultimate moment results, the reference specimens without joints gave an average value of 0.84 kNm, with a minimum of 0.61 kNm. For the members

with glued lap joints, the mean values of ultimate moment decreased to more than half (42%) of the reference specimens for top notches, and to 1/4 for bottom notches. Again, for bolted lap joints the reductions were even more pronounced, with the ultimate moment decreasing to 1/4 for upper-notches and to approximately 1/5 for bottom-notches.

The different joint configurations exhibited distinct failure modes. The reference specimens with full cross-section showed bending failure, characterized by tension failure parallel to the lower fibres (Fig. 12 left). In the case of upper-notch lap joints, bending at the reduced cross-section showed a similar typical failure mode. Details of this type of failure are illustrated in Fig. 13, viewed from below for both glued and bolted joints. However, a splitting failure mode occurred in members for bottom notches caused by tension perpendicular to the grain, with damage onset at very low load levels (Fig. 12 right).

The critical behaviour of the bottom-notch joints is also evidenced in the graphs presented in Fig. 11 right, where the minimum value of ultimate moment at which non-linearity begins is approximately 0.1 kNm.

The load F – deflection d relation of the four point bending tests can be translated into a semi-rigid rotational stiffness value with an equivalent analysis of two beams connected by a joint. The joint's stiffness k can then be obtained from the equation:

$$d = \frac{23}{1296}\frac{FL^3}{EI} + \frac{1}{12}\frac{FL^2}{k}$$

Although the number of tests is limited, they offer valuable insights into the effect of the joints on member behavior.

Structural analysis

The structural analysis of the tripod was performed as a second order linear elastic analysis using Finite Element Analysis (FEA) implemented in Karamba3D [20], with the base model shown in Fig. 14. The stiffness values for the semi-rigid joints stem from the joint tests and a sensitivity analysis was performed.

The structure is supported on its boundaries with pin connections. Based on preliminary studies, a design load of $G+A_r$ was considered as the most critical, with G the self-weight of the structure and A_r an accidental point load of 0.5 kN, applied in the outward radial direction, at human height, distributed over a set of adjacent nodes.

Three types of joints are considered, depending on the location on the beams and their reversibility (Fig. 7):

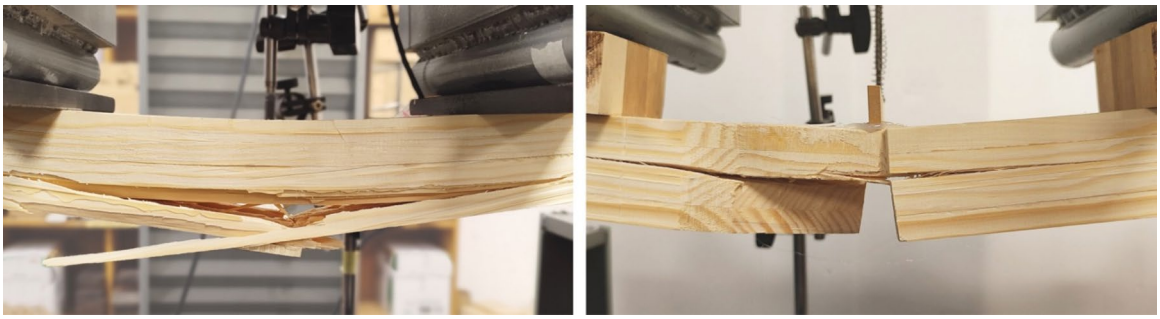

Fig. 12 Failure mode of specimens. Left: specimen without joint. Right: specimen with bottom notch

Fig. 13 Details of the failure mode of glued lap and bolted lap specimens with upper notch

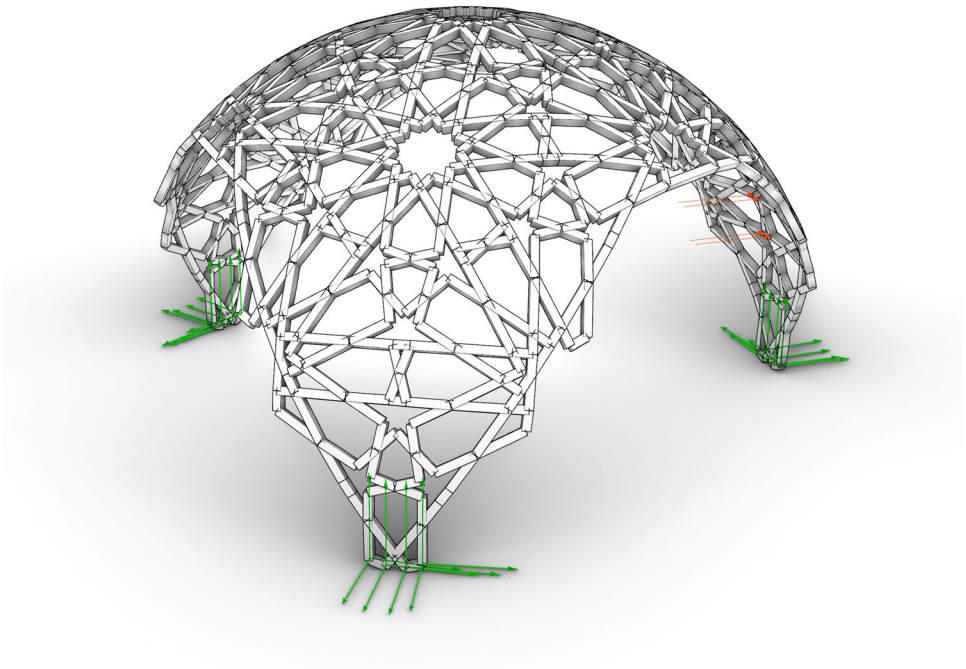

Fig. 14 Structural model of the Lazo tripod using FEA: geometry and boundary conditions

- Butt joints with a quasi-null rotational stiffness $k_b = 10^{-6}$ kNm/rad;
- Glued lap joints as semi-rigid joints with rotational stiffness $k_{lg,y} = 15$ kNm/rad;
- Screwed lap joints as semi-rigid joints with rotational stiffness $k_{lb,y} = 7$ kNm/rad.

In this study, the real hybrid distribution of glued and screwed lap joints is considered (modular dismountable), as well as the alternatives of screwed joints only (completely dismountable) and glued joints only (not dismountable). The translational and other rotational stiffnesses are considered infinite, assuming that bending in the weak direction of the joints drives the design of this structure. The parameters and results of the study are shown in Table 2.

The design with hybrid connection distribution (model 2) shows a maximum deflection of 2.6 cm, or 1/142 of the span L of 3.7 m, a high value but within the acceptable range for small deformation theory. The maximum compressive and tensile stresses in the beams are under 10 MPa, more than half below the acceptable material strengths. The moments at the connections are under 0.06 kNm in-plane and 0.08 kNm out-of-plane, under the recommended 0.1 kNm from the physical tests. The first buckling load factor is high, above 10, though connection failure will most likely occur before buckling failure due to the low plasticity of the structure. Figure 15 shows the deformed shape and the stress

Table 2 Results of numerical structural analysis of the tripod

Model number	1	2	3
Material elastic modulus E_0 [GPa]	15	15	15
$k_{ls,x}$ [kNm/rad]	10^6	10^6	10^6
$k_{ls,y}$ [kNm/rad]	7	7	15
$k_{ls,z}$ [kNm/rad]	10^6	10^6	10^6
$k_{lg,x}$ [kNm/rad]	10^6	10^6	10^6
$k_{lg,y}$ [kNm/rad]	7	15	15
$k_{lg,z}$ [kNm/rad]	10^6	10^6	10^6
Maximum deflection [cm]	3.3	2.6	2.5
First buckling load factor [-]	8.3	11.7	11.9
Maximum absolute in-plane bending moment [kNm]	0.049	0.056	0.057
Maximum absolute out-of-plane bending moment [kNm]	0.082	0.078	0.078
Highest compressive stress [MPa]	−9.76	−9.33	−9.37
Highest tensile stress [MPa]	9.89	9.49	9.54

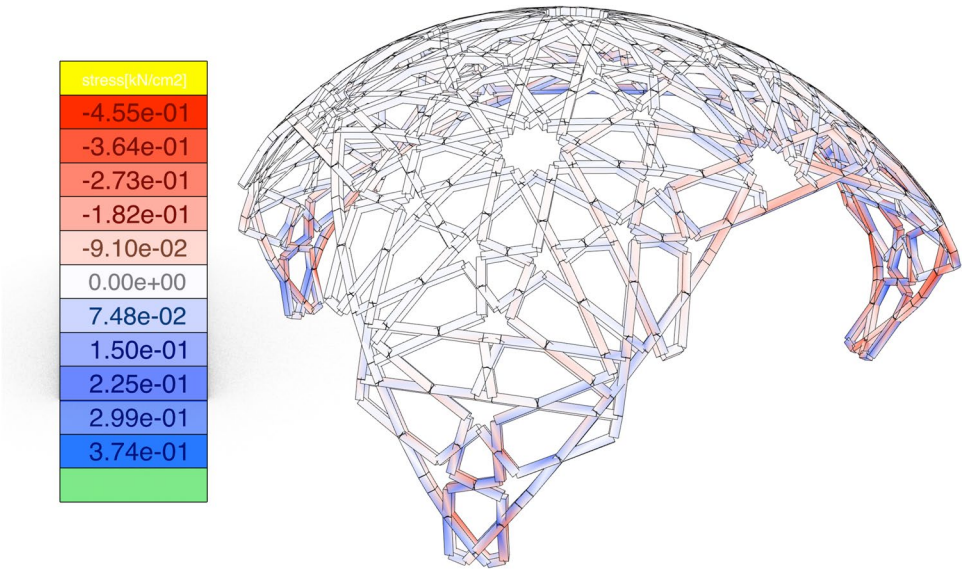

Fig. 15 Deformation mode and stress distribution of the tripod with hybrid glued and screwed lap joints. Stresses are shown in blue for tension and red for compression in a scale in kN/cm2

distribution in the tripod. For each design, flexibility through maximum deflection is the critical design aspect. Considering all-glued non-dismountable connections (model 3) decreases flexibility only to a maximum deflection of 2.5 cm (−4%). And considering all-screwed dismountable connections (model 1) increases flexibility to a maximum deflection of 3.3 cm (+27%), an unacceptable value higher than *L/100*.

As a summary, the hybrid distribution of joints allows partial dismountability into modules with little stiffness loss and without needing additional elements to stiffen the Lazo tripod, whereas a fully dismountable design would have led to an unacceptable stiffness.

Lazo tripod construction

Offsite manufacturing

The timber used in the making of the pavilion was sourced from a local pine lumberjack near Segovia (Spain). The timbers boards were was cut into laminas with a section of approximately 10 by 40 mm^2. To create the arched beam (*camón*), we constructed a mold from two MDF boards, shaped with curves matching the dome's radius. Four laminas were glued together and placed in the mold. In line with traditional craftsmanship, the lamina facing the intrados was painted at the center with a colored line (*gramil*), which enhances the interlacing effect between the timber elements.

The study by Candelas-Gutierrez [21] illustrates that certain *armadura* timber roof constructions were based on a bottom-up logic, skillfully combining and multiplying a simple unit—a straight rod element. While our design adheres to overall guidelines regarding the angle relationships between joint members (see Fig. 7), significant differences exist we did not utilize squares or *cartabones* in our approach. Nevertheless, the pavilion's reliance on modular elements ensures a high level of standardization, maintaining a bottom-up fabrication logic. The modular isosceles dome comprises two identical (but mirrored) sides and a base, resulting in three templates. From these templates, we can derive extended arms that branch from the isosceles, as well as the central hexagon (*aspilla triple*).

Conceptually, all curved elements of the pavilion can be traced back to the aforementioned three templates, with marking of the joinery. However, we tailored all templates and subtemplates to facilitate the fabrication process (see Fig. 16). These cardboard templates were created by unwrapping the interior faces of the curved elements from the 3D model and were cut using a laser. Once the joints were traced and cut, the carpenter assembled the isosceles unit. This assembly involved adjusting the joints between elements through sawing and clamping. After completing the adjustments, the joints within each isosceles unit were glued and fixed in place. The joints between the triangles were left unglued and instead utilized a bolt-and-nut system to allow for disassembly of the structure. After marking the lines of the joints on the intrados of the dome, we used a jig to approximate the radial lines on the sides of the *camón*, which helped outline the entire joint on the curved beam (Fig. 17).

The construction of the modular pavilion involved creating both the dome and the tripod structure derived from it (Fig. 5, Fig. 18). The dome was composed of 35 triangles, while the tripod required 18 triangles, two of which were specifically designed for the tripod and were not part of the dome. This resulted in a total of 37 spherical triangles. Each spherical triangle has approximate dimensions of 1.34 m for the base and 1.2 m for the sides. The average time of making one spherical triangle from scratch to final preparation was about two full days, which equals 16 h.

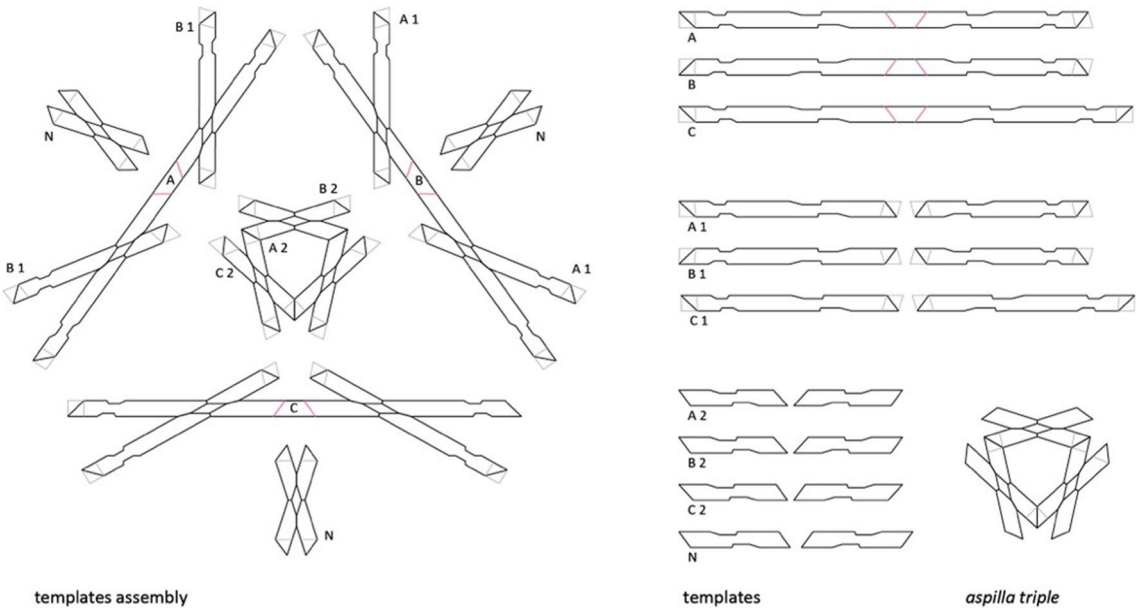

Fig. 16 The templates layouts for the marking and tracing of the joinery

Fig. 17 The process of creating a spherical triangle from top left to bottom right**:** preparing the pinewood laminas, molding them into curved elements, the resulting curved element, tracing joints using templates, cutting the joints, and the final curved elements carved joints

On-site assembly

The pre-assembly of the pavilion occurred in the workshop during the fabrication of the individual units, which was essential for two main reasons. First, it allowed for adjustments of the joineries between the units and the installation of screws and bolts. Second, it provided an opportunity to strategize the sequence of installation for the dome. The

Fig. 18 The process of assembling the spherical triangles in the workshop. Left, a typical spherical triangle. Right: assembling part of the pavilion

workshop assembly process was replicated on-site. The assembly sequence for the dome progressed from top to bottom. The upper center of the tenfold rosette (the pentagon) was suspended from a crane, a crucial method that created space for maneuvering while adding the triangles to the structure. This approach would have been far more challenging had the assembly begun from the lower parts upward, as the structure would have deformed and made closing the dome with the 'keystone' module difficult.

Each connection between two triangles involved six joineries: two at the center of their pair of shared rosettes and two at their extending arms. Because the lap joints alternated in direction, one of the two triangles had to be twisted during installation (Fig. 8, Fig. 19). The carpenters relied on the natural flexibility of wood to carefully squeeze and interlace the sides of the triangle. For the first pentagon, the triangles were assembled in a clockwise sequence. However, when closing the pentagon—where the first and

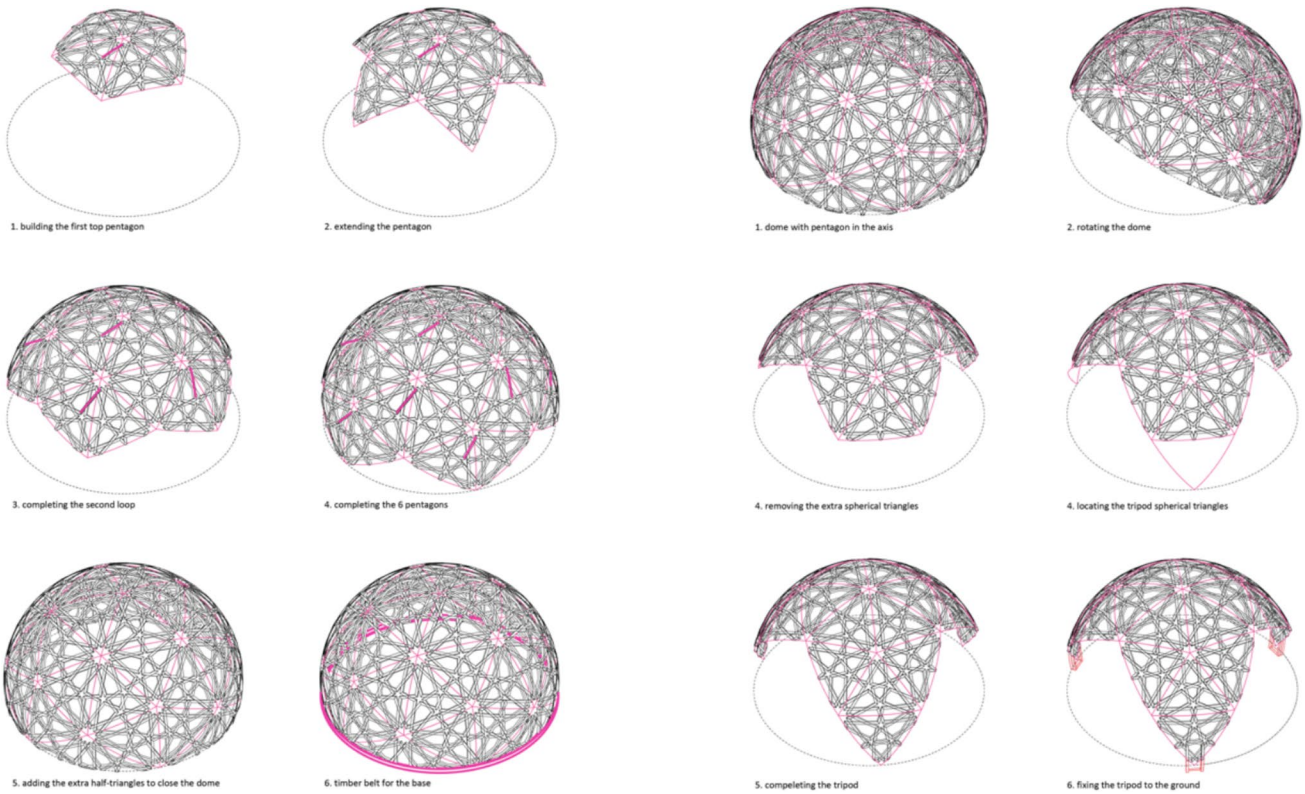

Fig. 19 On-site assembly sequence. Left: the making of the full dome with the pentagon at the apex. Right: the transfer from the dome to the tripod pavilion with the hexagon at the apex

last triangles meet—the usual squeezing technique was not feasible (Fig. 19). To address this, one of the two triangles had to be modified, with one of its arms crafted in two separate pieces (a top one and a bottom one) to clamp the adjoining triangle. This clamping method was repeated at various locations where triangles met, closing the loops of the assembly. For the dome, the lower five triangles located at the closing ring were added, and a timber belt closed the dome. After the construction of the dome, a transformation occurred to transition it into the tripod pavilion. First, several triangles were removed and stored, and the axis of the sphere was also adjusted, as the tripod features a hexagon at its apex rather than a pentagon like the dome. Then, the spherical triangles for the legs were added to the structure, and, finally, the tripod was fixed onto steel supports (see Fig. 18 right and Fig. 19) (see Fig. 20).

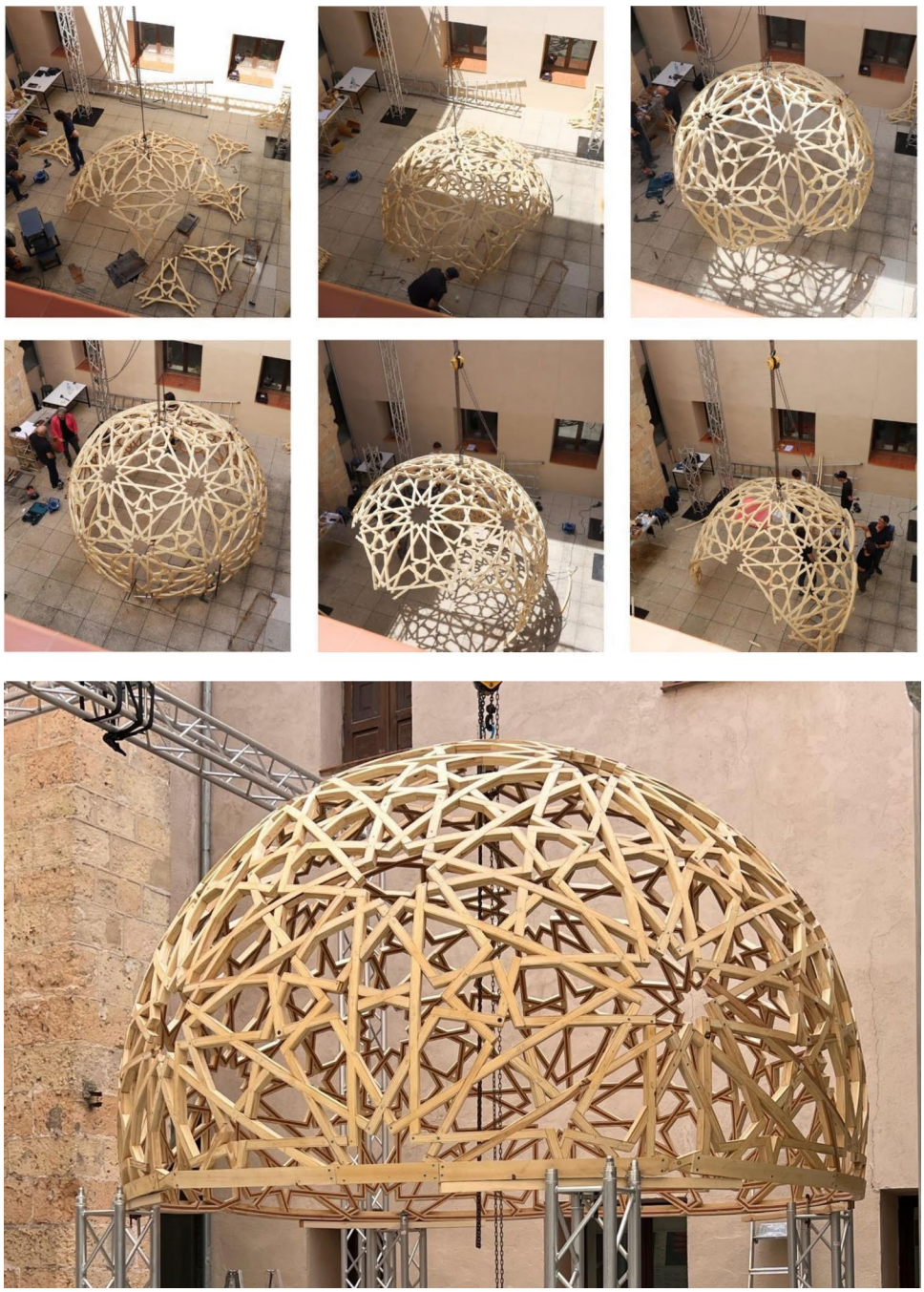

Fig. 20 On-site assembly of the dome and converting it into the tripod pavilion

Conclusion

This paper presents an applied study on the construction and development of structural timber domes, grounded in Spanish traditional carpentry, *Carpintería de lo Blanco*, and adapted within contemporary architectural methods (Fig. 21). Beginning with a survey of historical examples that explore the interplay between spherical surfaces and Islamic geometries, the study analyzes a set of solutions for polyhedral projections onto spherical surfaces. Using the pentakis dodecahedron as a base geometry—chosen for its repetitive isosceles triangular faces—the study establishes this triangle as a modular unit for constructing a pavilion derived from a spherical form. By integrating the traditional *lazo* (strapwork) design within this projection, the research brings together principles from traditional *Lazo* timber construction

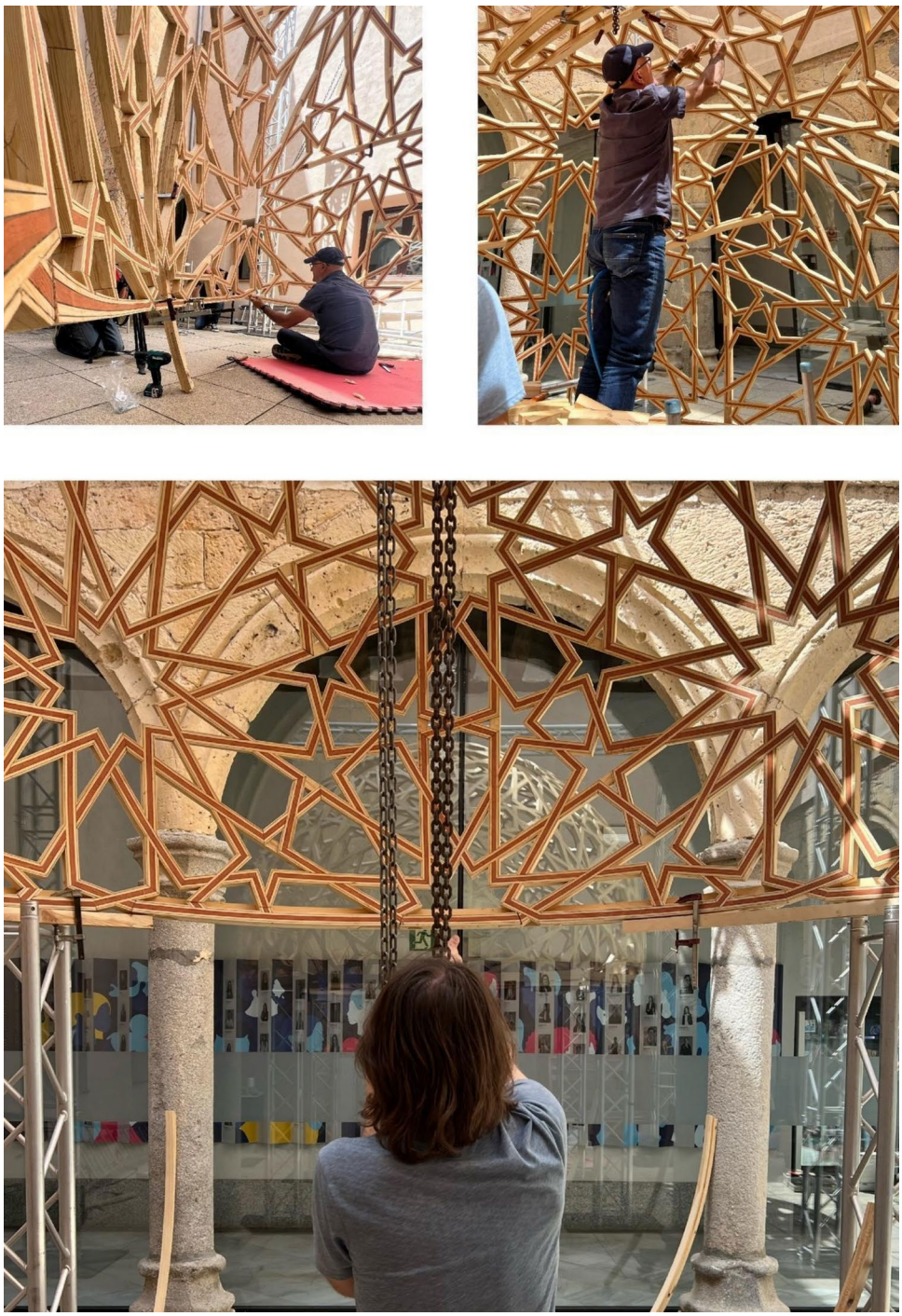

Fig. 21 Details of assembly of the Lazo dome and pavilion. Top left: installing the lower belt. Top right: installing the *apsilla* with nails. Bottom: the crane system of the assembly of the dome

Fig. 22 Lazo Pavilion

with new aspirations for modular assembly, disassembly, and unification of ornamental and structural elements. The paper refers to these new conditions as *structural Lazo* (Fig. 22).

To achieve a structural *Lazo*, the research generated a strategy of half-lap joinery, ranging from fixed glued joints to reconfigurable bolt-and-nut joints. Through mechanical testing of joints and material samples alongside Finite Element Analysis (FEA), the study evaluated the structural behavior of a four-meter-span *Lazo* pavilion. The construction of this demonstrator pavilion provided insights into the fabrication of modular units (spherical triangles) and their systematic assembly.

This study represents an initial exploration into contemporary potentials for traditional timber domes designed for both permanent and flexible applications, emphasizing the synergy between Islamic ornamental geometry and structural performance. It opens new pathways for further studies on the relationship between polyhedral geometry and Islamic patterns within timber craftsmanship, for both spherical and non-spherical surfaces. Structurally, the study suggests avenues for exploring material choices beyond the used softwood, *Pinus sylvestris*, as well as further investigation into joinery types in this genre of timber construction, especially if scaled for larger applications in grid-shell timber domes. Insights from the pavilion's construction revealed that an assembly strategy starting from the top and working downward was more successful than the reverse. Further exploration of alternative assembly strategies could consider the reciprocal behavior of spherical triangles during assembly.

Finally, on an interdisciplinary level, this paper highlights collaboration among architects, engineers, and craftspeople. Building upon the extensive research of the master carpenter, who pioneered work in spherical timber domes, this project further explores their full-scale construction, structural behavior, and modularity. Future research and projects of this nature can uncover innovative intersections between historical construction techniques and modern architectural applications.

Acknowledgements This project builds on Ángel María Martín López's intensive research into new solutions for spherical timber Lazo domes and his development of polyhedral projection on spherical surfaces for Lazo dome. The team is grateful to the technical staff at IE University for their support in the dome's installation.

Author contribution A.M.L is the lead designer and builder of the case study. W.A coordinated and wrote the main text and prepared Figs. 1–2, 5–12, 16–22. O.G wrote Sects. 1.2 and 2.1, and O.G and W.A prepared Figs. 3,4. A.L,A.M wrote Sect. 3.1 and prepared Figs. 9–13 and Table 1. R.O wrote Sect. 3.2 and prepared Figs. 14,15 and Table 2. All authors reviewer the manuscript. R.O is the lead of the FEA modeling and analysis. A.L and A.M are the leads of samples physical analysis. W.A and S.A directed and coordinated the research operations and secured funding.

Funding This work was supported by the Princeton Faculty Fund.

Data availability No datasets were generated or analysed during the current study.

Declarations

Competing interests The authors declare no competing interests.

References

1. Nuere E (2017) La carpintería de armar española, inicio de la prefabricación en la arquitectura. Mater Arquit 15:32–43

2. Nuere E (2001) Nuevo tratado de la carpintería de lo blanco y la verdadera historia de Enrique Garavato, carpintero de lo blanco y maestro del oficio. Munillalería, Madrid
3. de Mingo García J, Fernández-Zúñiga MS (2023) Apuntes de Carpinteria de Armar Española.
4. Aljazairi López G (2010) La carpintería de lo blanco, teoría, traza y reproducción: las cubiertas de lazo del convento de La Merced. Universidad de Granada. http://purl.org/dc/dcmitype/Text
5. Grünbaum B, Shephard GC (1987) Tilings and patterns. Courier Dover Publications
6. Bonner J (2017) Islamic geometric patterns. Springer, New York, NY. https://doi.org/10.1007/978-1-4419-0217-7
7. Cromwell PR (2009) The search for quasi-periodicity in Islamic 5-fold ornament. Math Intell 31:36–56. https://doi.org/10.1007/s00283-008-9018-6
8. Nejad Ebrahimi A, Azizipour Shoubi A (2020) The Projection Strategies of Gireh on the Iranian Historical Domes. Math Interdiscip Res 5. https://doi.org/10.22052/mir.2020.212903.1187
9. Matauco EN, Candelas-Gutierrez Á, de García JM (2020) Análisis constructivo de la cúpula de madera del desaparecido Palacio de los Cárdenas en Torrijos (S.XV). Inf Constr 72:e353–e353. https://doi.org/10.3989/ic.71019
10. de Mingo García J, María Martín Á (2021) Cúpulas en la carpintería de lazo: Historia, trazado y propuesta de desarrollo con la geometría esférica y las normas del oficio como base. J Tradit Build Archit Urban 290–304
11. Popko ES, Kitrick CJ (2021) Divided Spheres: Geodesics and the orderly subdivision of the Sphere, 2nd edn. A K Peters/CRC Press. https://doi.org/10.1201/9781003134114
12. Kaplan CS (2017) Interwoven Islamic Geometric Patterns. Proceedings of Bridges 2017: Mathematics, Art, Music, Architecture, Education, Culture, pp 71–78. https://archive.bridgesmathart.org/2017/bridges2017-71.html#gsc.tab=0.ISBN978-1-938664-22-9
13. Makovicky E, Fenoll Hach-Alí P (2000) Structure of the domes of pavilions in the Patio de los Leones, the Alhambra: a distorted octacapped truncated octahedron. Boletin Soc Espanola Mineral 23:37–41
14. Centro de Interpretacion de la Carpinteria Mudejar de la Morana (n.d.) Available at: https://www.xn--carpinteriamudejardelamoraa-fvc.com/. Accessed 7 Mar 2025
15. Gáspár O (2022) The optimization process leading to the tessellation of the first geodesic dome structure, the first Planetarium of Jena. Int J Space Struct 37:49–64. https://doi.org/10.1177/09560599211064110
16. Lara-Bocanegra AJ, Majano-Majano A, Ortiz J, Guaita M (2022) Structural analysis and form-finding of triaxial elastic timber gridshells considering interlayer slips: numerical modelling and full-scale test. Appl Sci 12:5335. https://doi.org/10.3390/app12115335
17. Branco JM, Descamps T (2015) Analysis and strengthening of carpentry joints. Constr Build Mater 97:34–47. https://doi.org/10.1016/j.conbuildmat.2015.05.089
18. Meisel A, Moosbrugger T, Schickhofer G (2010) Survey and Realistic Modelling of Ancient Austrian Roof Structures: 3rd International Workshop on Civil Structural Health Monitoring. Conserv Herit Struct, pp 481–494
19. UNE-EN 408:2011+A1:2012 Timber structures. Structural timber and glued laminated timber
20. Preisinger C, Heimrath M (2014) Karamba—a toolkit for parametric structural design. Struct Eng Int 24:217–221. https://doi.org/10.2749/101686614X13830790993483
21. Candelas-Gutierrez A (2017) The power of geometric relationships in mudéjar timber roof frames. Nexus Netw J 19:521–545. https://doi.org/10.1007/s00004-017-0340-1